Mammal Research (2018) 63:277–283
https://doi.org/10.1007/s13364-018-0364-2

ORIGINAL PAPER

Differentiation of craniomandibular morphology in two sympatric *Peromyscus* mice (Cricetidae: Rodentia)

Kaz Jones[1] · Chris J. Law[1]

Received: 20 December 2017 / Accepted: 8 March 2018 / Published online: 20 March 2018

Abstract

In the Santa Cruz Mountains of California, dietary partitioning is believed to allow *Peromyscus californicus* (California mouse) and *Peromyscus truei* (pinyon mouse) to occur sympatrically; *P. californicus* feeds primarily on arthropods, whereas *P. truei* feeds primarily on acorns. To better understand how these species partition resources, we examine if these dietary differences extend to differences in craniomandibular morphology. We use a geometric morphometric approach to test the hypothesis that *P. californicus* and *P. truei* exhibited size and shape differences in craniomandibular morphology, in particular, regions of the skulls that pertain to biting ability and mechanical advantage of the jaw adductor muscles. We found that *P. truei* exhibited relatively wider zygomatic arches, relatively broader, more robust masseteric fossa and coronoid process, and a higher mechanical advantage of the masseter jaw muscle. These craniomandibular traits suggested that *P. truei* exhibits a relatively stronger bite force that is more suitable to access hard-shelled acorns despite its smaller body size.

Keywords Bite force · Dietary partitioning · Geometric morphometrics · Mechanical advantage · Skull morphology

Introduction

Closely related species often share morphological and functional characteristics that allow them to fall within the same ecological guild and use the same resources in similar ways (Root 1967; Schoener 1974; Dayan and Simberloff 1994). However in zones of sympatry, high interspecific competition is expected to drive resource partitioning between these ecologically similar species resulting in separation of ecological niches such as space use, time, and/or diet (Pianka 1973; Schoener 1974). Accompanying niche partitioning is differentiation of the underlying morphology/physiology, behavior, and performance that facilitates exploitation of specific resources for each species (Verwaijen et al. 2002; Mori and Vincent 2008; Žagar et al. 2017). This ecomorphological paradigm elucidates the interactions between sympatric species and their environments (Wainwright 1991; Ferry-Graham et al. 2002; Grant and Grant 2002), which in turn provides better understanding of the mechanisms that shape species coexistence.

As the most populous native mammals in North America, deer mice (genus *Peromyscus*) range across a variety of ecosystems and frequently share overlapping habitats between two or three *Peromyscus* species (Kaufman and Kaufman 1989). Extensive studies on niche partitioning between sympatric deer mice have found that differences in dietary preference may be one of the primary mechanisms that reduce interspecific competition (Smartt 1978; Kalcounis-Rüppell and Millar 2002; Reid et al. 2013). Researchers have also examined the morphological, behavioral, and functional differences that underlie differences in the exploitation of prey. In most mammals, the ability to exploit particular prey is limited by the biting ability generated by craniomandibular morphology (Kardong 2014). Therefore, the ecomorphological paradigm hypothesizes a strong link between craniomandibular morphology and prey exploitation. Previous studies with lizards, turtles, birds, and mammals have revealed that variation in craniomandibular morphology can influence dietary profitability by expanding/limiting the food items accessible to a

Communicated by: Joanna Stojak

Electronic supplementary material The online version of this article (https://doi.org/10.1007/s13364-018-0364-2) contains supplementary material, which is available to authorized users.

✉ Chris J. Law
cjlaw@ucsc.edu

[1] Department of Ecology and Evolutionary Biology, University of California, Coastal Biology Building, Santa Cruz, 130 McAllister Road, Santa Cruz, CA 95060, USA

predator and increasing/decreasing prey handling time (Herrel et al. 2001; Verwaijen et al. 2002; Herrel et al. 2006; van der Meij and Bout 2006; Bulté et al. 2008). Furthermore, closely related sympatric vertebrates exhibit different craniomandibular morphologies that facilitate dietary partitioning by allowing each species to specialize on different prey items (Verwaijen et al. 2002; Mori and Vincent 2008; Santana et al. 2010). These shifts toward different craniomandibular morphologies, however, are not only driven by evolutionary processes but may also be driven by developmental plasticity. A plethora of studies have demonstrated that differences in dietary consistency can affect the shape of the skull and dental morphology (Watt and Williams 1951; Myers et al. 1996; Maki et al. 2002).

In this study, we examine if the dietary partitioning observed between two sympatric *Peromyscus* mice are accompanied by differences in craniomandibular morphology. *Peromyscus californicus* (California mouse) and *Peromyscus truei* (pinyon mouse) occur sympatrically in the Santa Cruz Mountains and can be distinguished primarily by mean body mass where *P. californicus* (43.04 g) is larger than *P. truei* (26.92 g) (SMURF, unpublished data). Recent isotopic analyses revealed dietary differences between these two species (Reid et al. 2013): *P. truei* (misidentified as *Peromyscus boylii* in Reid et al. 2013) primarily specializes on tanoak acorns (*Notholithocarpus densiflorus*) during the winter, spring, and summer months and Shreve oak (*Quercus parvula*) and California live oak (*Quercus agrifolia*) acorns in the fall. In contrast, *P. californicus* feeds at a higher trophic level and primarily consumes spiders (Araneae) in addition to beetles (Coleoptera), crickets (Orthoptera), and some supplementary acorns from *N. densiflorus* and *Q. parvula* (Reid et al. 2013). To better understand the link between dietary partitioning and craniomandibular variation, we test the hypothesis that *P. truei* and *P. californicus* exhibit differences in craniomandibular size and shape as well as mechanical advantage of the jaw adductor muscles. We predict that *P. truei* will exhibit relatively wider zygomatic arches, more robust mandibles, and greater mechanical advantage that can facilitate relatively stronger biting ability needed to specialize on hard-shelled acorns.

Materials and methods

Specimens and geometric morphometric superimposition We quantified differences in the cranium and mandible by analyzing three views of the skull with 2D landmark-based geometric morphometrics (Rohlf and Slice 1990; Zelditch et al. 2012). We obtained 41 adult *P. californicus parasiticus* skulls (16 females, 25 males) and 33 adult *P. truei dyselius* skulls (15 females, 18 males) from the mammal collection at the California Academy of Sciences (Supplementary Data 1). Specimens originated from the Santa Cruz Mountains within Santa Clara and Santa Cruz counties in California. All specimens were fully mature, determined by the complete eruption of all cheek teeth (Holmes et al. 2015).

Each specimen was photographed in three views: (1) cranium in ventral view, photographed by orienting the palate plane parallel to the photographic plane; (2) cranium in lateral view, photographed by orienting the midsagittal plane parallel to the photographic plane; and (3) mandible in lateral view, photographed by orienting the long axis of the dentary parallel to the photographic plane. Photographs were taken using a Canon 70D DSLR camera affixed to a Kaiser 205513 RS-10 copy stand kit. Specimens were placed at a distance of 35 cm away from the camera lens. A ruler with 1 × 1 cm grids was used to ensure no distortion as well as serve as a scale bar.

Fig. 1 Landmarks (large black circles) and semi-landmarks (small red circles) used for geometric morphometric analysis of skull shape and size. Specimen is a male *Peromyscus californicus* (CAS MAM 12567). The scale bar represents 1 cm of distance. **a** Ventral cranial view: (1) anteriormost point of the suture between nasals, (2) and (3) lateralmost point of the alveolus of the incisor, (4) and (5) lateral tip of the incisor, (6) and (7) anteriormost point of the incisive foramen, (8) and (9) exterior ends of the premaxillary-maxillary sutures, (10) and (11) lateralmost extent of suture between the premaxilla and maxilla, (12) and (13) anterodorsal tip of zygomatic plate, (14) and (15) posteriormost point of the incisive foramen, (16) and (17) anteriormost point of the orbit, (18) and (19) anteriormost point of the molar row, (20) and (21) lateral paracone of first molar, (22) and (23) contact point between first and second molars, (24) and (25) contact point between second and third molars, (26) and (27) posteriormost point of the third molar, (28) and (29) least post-palatal distance across the palatines, (30) and (31) anteriormost point of the glenoid fossa, (32) and (33) posterior end of squamosal root of zygomatic bar, (34) posteriormost extent of palate at the midline, (35) and (36) suture between basisphenoid and basioccipital at point of contact with the auditory bulla, (37) and (38) lateral margins of the foramen ovale, (39) anteriormost point of the foramen magnum along the midline, (40) posteriormost point of the foramen magnum on the midline, (41) and (42) lateral margins of the foramen magnum, (43) and (44) posteriormost margin of the mastoid process. **b** Lateral cranial view: (1) posteriormost point of the upper incisive alveolus, (2) inferiormost point of the upper incisive alveolus, (3) interior most point of suture between nasal and premaxillary, (4) anterior tip of the nasal, (5) curvature at the limit between the occipital condyle and the occipital bone, (6) inferior extremity on the boundary between the occipital condyle and the tympanic bulla, (7) ventral-most point of the interior of the opening to the tympanic bulla, (8) dorsal-most point of the interior of the opening to the tympanic bulla, (9) posteriormost point of the molar row, (10) anteriormost point of the molar row, (11) ventral extent of the suture between maxilla and premaxilla, (12) anteriormost point of the orbit, (13) anteriormost point of the glenoid fossa in the zygomatic bar, (14) posterior end of zygomatic bar. **c** Mandibular view: (1) anteroventral border of incisive alveolus, (2) upper extreme anterior border of incisor alveolus, (3) position of greatest inflection of the diastema, (4) Anterior edge of the alveolus of first molar, (5) intersection between molar crown and coronoid process in lateral view, (6) tip of the coronoid process, (7) point of maximum curvature between the coronoid and condylar process, (8) dorsal margin of the anterior edge of the articular surface of the condylar process, (9) ventral edge of the articular surface of the condylar process, (10) point of maximum curvature between condylar and angular process, (11) tip of the angular process, (12) intersection between mandibular body and masseteric crest

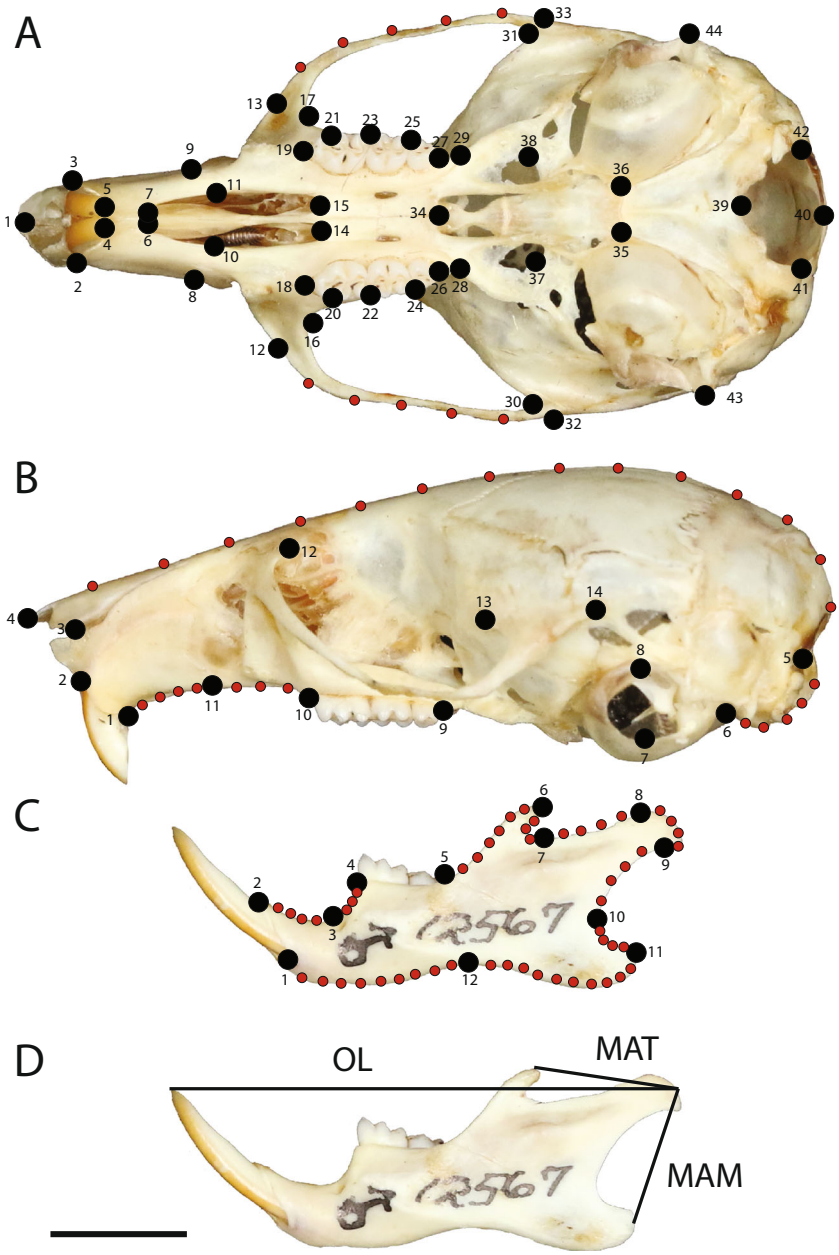

We then placed homologous morphological landmarks and semi-landmarks on the lateral cranial, ventral cranial, and lateral mandibular views. We used 14 landmarks and 26 semi-landmarks on the lateral cranial view, 44 landmarks and 10 semi-landmarks on the ventral cranium view, and 11 landmarks and 51 semi-landmarks on the lateral mandibular view (Fig. 1) based on Maestri et al. (2016). Landmarks were chosen for their potential to be recognized across a species; semi-landmarks were generated at evenly spaced intervals between landmarks. All landmarks were digitized using the program tpsDig-v 2.30 (Rohlf 2005). We then aligned digitized specimens using a generalized Procrustes superimposition (Rohlf and Slice 1990) in the R package geomorph 3.0.1 (Adams and Otárola-Castillo 2013) in R 3.2.1 (R Core Team 2017). During the Procrustes superimposition, semi-landmarks on the curves were allowed to slide along their tangent vectors until their positions minimized bending energy (Bookstein 1997; Zelditch et al. 2012). After superimposition, bilaterally homologous landmarks on the ventral cranium were reflected across the midline and averaged using the geomorph function *bilat.symmetry*.

Analysis of skull size and shape We first examined if sexual dimorphism in skull size and shape was significant within each species. For each species, we determined if the size of each skull view was significantly different between the sexes using separate analyses of variance (ANOVAs) on the centroid size of each configuration of landmarks (the square root of the

sum of the squared distances from each landmark to the geometric center of the shape) (Bookstein 1997). Similarly, we determined if skull shape within each species was significantly different between the sexes using a Procrustes ANOVA (Goodall 1991; Anderson 2001) with a factorial design on each of the skull view datasets. For each skull view, we used shape as the dependent variable, sex as the main factor, and centroid size as a covariate.

We found no significant sexual dimorphism in size or shape of any skull view; therefore, we pooled males and females in our analyses of interspecific differentiation. For each skull view, we examined differences in skull size and skull shape using ANOVAs and Procrustes ANOVAs, respectively. Procrustes ANOVAs were conducted with a factorial design with shape as the dependent variable, species as the main factor, and centroid size as a covariate. Procrustes ANOVAs were performed with the procD.lm function in the R package geomorph 3.0.1 (Adams and Otárola-Castillo 2013). We also used a pairwise permutation test with the permudist function in the R package MORPHO 2.4 (Schlager 2016) to quantify shape differences (Procrustes distances) between the two species and to determine if these differences were significant. Lastly, we performed separate principal component analyses on the Procrustes coordinates of each skull view to visualize the tangent space (form) of the two species.

Mechanical advantage We assessed differences in biting ability between the two species by modeling the lower jaw as a lever and calculating mechanical advantage (MA) of the temporalis and masseter masticatory muscles (e.g., Tanner et al. 2010; La Croix et al. 2011; Timm-Davis et al. 2015; Law et al. 2016a). MA describes the proportion of jaw muscle force transmitted to the bite point; relatively higher MA indicates higher force-modified jaws (Kardong 2014). MA is calculated as the ratio between the in-lever, the distance between the mandibular condyle and the muscle insertion point, and the out-lever (OL), the distance from the mandibular condyle to the tip of the incisor. We used moment arm of temporalis (MAT), measured from the tip of the coronoid process to the condyle, and moment arm of masseter (MAM), measured from the tip of the angular process to the condyle, as our temporalis and masseter in-lever (moment arm) distances, respectively. The out-lever was measured to the tip of the incisor (Fig. 1d). Shapiro–Wilk tests indicated that MA exhibited a normal distribution. Thus, we performed ANOVAs to determine whether there were significant sexual differences in MA.

Results

Skull size and shape Skulls of the *Peromyscus californicus* were significantly larger than skulls of the *P. truei* in the ventral cranium ($F_{1,72} = 155.16$, $P < 0.001$), lateral cranium ($F_{1,72} = 4726$, $P < .001$), and mandible ($F_{1,72} = 4726$, $P < 0.001$). A principal component analysis of the Procrustes coordinates revealed form of all three skull views largely separated out between the two species on PC1 (Fig. 2). Analyses with both Procrustes ANOVAs and pairwise permutation tests confirmed significant shape differences for all three skull views (Table 1; Fig. 3). In the cranium, the *P. truei* exhibited relatively longer tooth rows, relatively wider zygomatic arches, and relatively longer dorsal cranial profiles (Fig. 3a, b). In the mandible, the *P. truei* exhibited relatively broader, more robust masseteric fossa and coronoid process but exhibited a relatively shorter angular process (Fig. 3c).

Procrustes ANOVAs also revealed significant allometry between shape and size in the crania of both species; however, these allometric patterns do not significantly differ between the two species (Table 1). The mandible, in contrast, does not exhibit significant allometry between mandibular shape and size (Table 1).

Mechanical advantage Feeding performance was measured as the MA of the two primary jaw adductor muscles, the temporalis and masseter muscles. MA of the temporalis did not differ significantly between the two species ($F_{1,72} = 0.442$, $P = 0.508$). In contrast, *P. truei* exhibited significantly greater MA of the masseter compared to *P. californicus* ($F_{1,72} = 21.69$, $P < 0.001$).

Discussion

Within the Santa Cruz Mountains, *Peromyscus truei* and *P. californicus* are congeners that coexist in sympatric locations. Their ability to coexist is hypothesized to be a result of dietary niche partitioning: *P. truei* specializes on hard-shelled acorns, whereas *P. californicus* primarily feeds on arthropods such as Araneae, Orthoptera, and Coleoptera (Reid et al. 2013). Consistent with these dietary differences, we found craniomandibular differences that allow *P. truei* to be better suited to process hard-shelled acorns compared to *P. californicus*. Specifically, we found that *P. truei* exhibited relatively wider zygomatic arches and relatively longer rostrum in the cranium and relatively broader mandibular ramus. These traits serve as attachment sites for the masticatory muscles, particularly the masseter that originates at the zygomatic arch, spans across the mandibular ramus, and inserts at the angular process (Turnbull 1970; Cox 2008). As the largest of the masticatory muscles in rodents, the masseter exerts the strongest force during jaw closure (Turnbull 1970) and increases bite efficiency at the incisors (Druzinsky 2010). Therefore, the relatively wider zygomatic arches and broader mandibular rami found in *P. truei* suggest relatively larger masseter muscles and thus relatively greater biting ability than *P. californicus*.

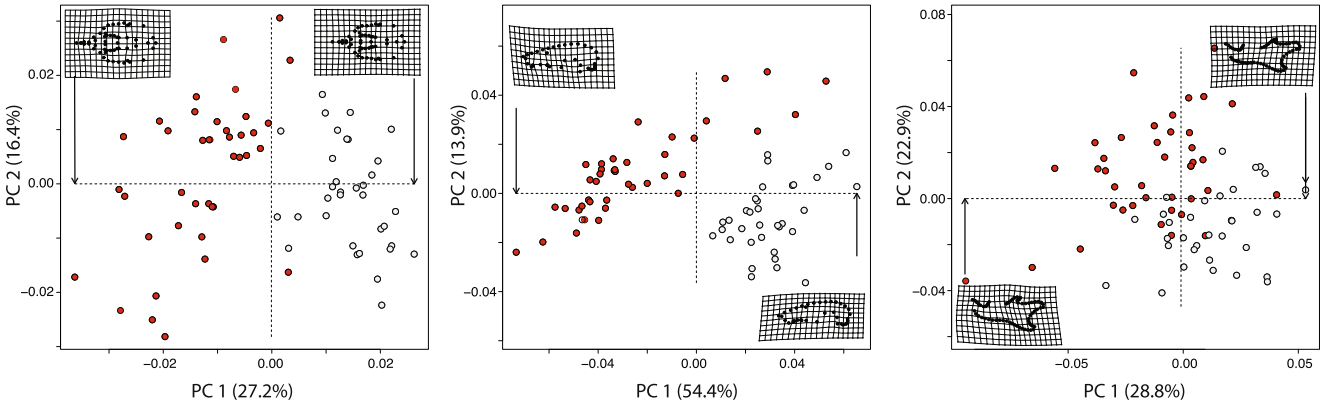

Fig. 2 Principal components plot of skull form variation. Deformation grids display shapes at the ends of the range of variability along PC1 (red = *P. truei*, light gray = *P. californicus*). Shapes of all three skull views are significantly different between the two species (Table 1)

Our finding that *P. truei* also exhibits greater MA of the masseter further corroborates these morphological differences. Higher MA is typically associated with increased force-modified jaws (Kardong 2014) that are adapted to process hard-shelled prey. Unsurprisingly, relatively higher MA of the masticatory muscles are found in several durophagous vertebrates such as loggerhead musk turtles (Pfaller et al. 2011), some moray eels (Collar et al. 2014), and southern sea otters (Law et al. 2016b).

Together, our analyses of the craniomandibular morphology and mechanical advantage suggest that, for a given size, *P. truei* exhibits relatively greater bite force than *P. californicus*. These biomechanical differences in the feeding apparatus often correspond to realized dietary differences in sympatric species (Verwaijen et al. 2002; Mori and Vincent 2008; Santana et al. 2010). Because the force an animal can generate by biting limits the range of prey items it can consume, greater bite forces strongly correlate with reduced handling times for both prey capture and consumption (Herrel et al. 2001; van der Meij and Bout 2006; Anderson et al. 2008) and the ability to expand dietary breadth by consuming larger or more robust food items (Verwaijen et al. 2002; Herrel et al. 2006; Bulté et al. 2008; Pfaller et al. 2011). In the Santa Cruz Mountains, a relatively greater bite force allows *P. truei* to consume hard-shelled acorns at a greater efficiency than *P. californicus* despite its smaller body size. Nevertheless, the phenomenon of many-to-one mapping of morphology to function has demonstrated that different morphological traits

Table 1 Results from Procrustes ANOVAs for species differences in cranial and mandibular shape

	SS	MS	R^2	$F_{1, 70}$	*P* value
A. Ventral cranium					
Species	0.014431	0.014431	0.216963	20.4789	*0.001*
Centroid size	0.003063	0.0030635	0.046058	4.3474	*0.001*
Species × size	0.000396	0.0003964	0.00596	0.5626	0.873
Residuals	0.048623	0.0007047			
Total	0.066513				
B. Lateral cranium					
Species	0.06164	0.06164	0.35627	41.5693	*0.001*
Centroid size	0.0064	0.0064	0.03699	4.3161	*0.005*
Species × size	0.001178	0.001178	0.00681	0.7943	0.517
Residuals	0.103797	0.001483			
Total	0.173014				
C. Mandible					
Species	0.025682	0.0256825	0.143532	12.1203	*0.001*
Centroid size	0.00385	0.0038498	0.021515	1.8168	0.064
Species × size	0.001073	0.0010731	0.005997	0.5064	0.859
Residuals	0.148327	0.002119			
Total	0.178932				

Italicized *P* values indicate significance ($\alpha = 0.05$)

SS sum of squares, *MS* means squares

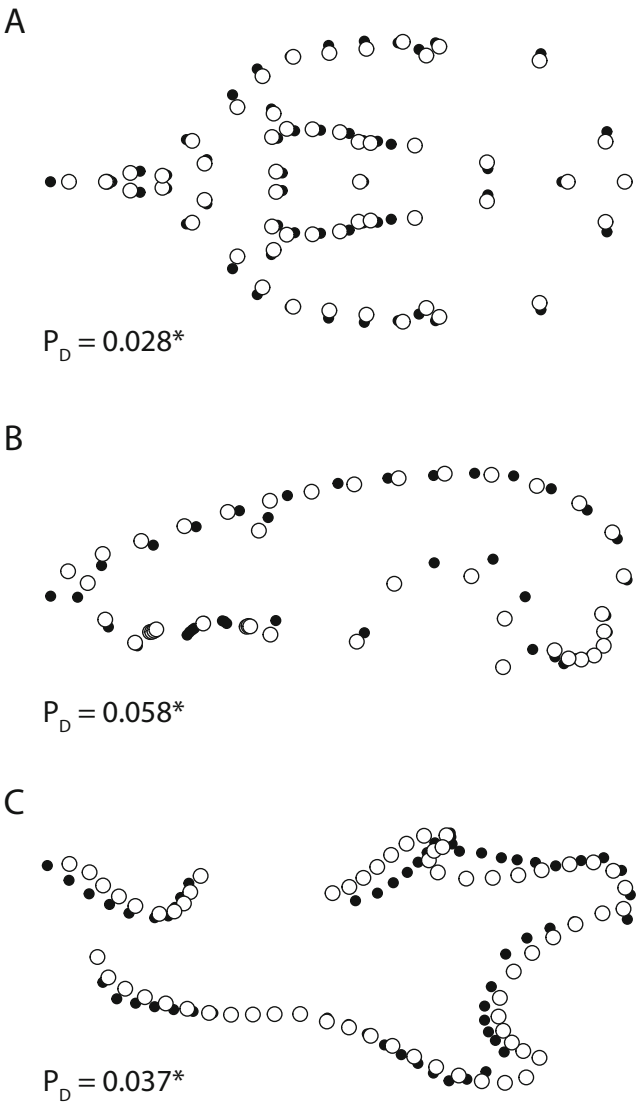

Fig. 3 **a**–**c** Differences in mean shapes (Procrustes distances) between *P. californicus* (large white circles) and *P. truei* (small black circles). Differences were magnified by a factor of 2 to display shape differences between the two species. P_D = Procrustes distance between mean shape of California mouse and *P. truei*. Asterisks "*" indicate significant P_D based on pairwise permutation test

will not necessarily translate to different functional traits (Alfaro et al. 2005; Wainwright et al. 2005). Therefore, whether these differences in craniomandibular morphology between *P. californicus* and *P. truei* results in actual differences in in vivo bite forces will requires further investigation.

Conclusion

Here, we found that *P. truei* exhibits craniomandibular morphology (relatively wider zygomatic arches in the cranium and relatively broader mandibular rami) better suited to process hard-shelled acorns along with higher mechanical advantage of the masseter jaw muscle relative to *P. californius*. Although these findings are consistent with the dietary differences exhibited by *P. truei* (acorn specialist) and *P. californicus* (arthropods), the underlying mechanisms that led to these morphological differences are not yet clear. Several confounding factors not analyzed in this present study may drive these differences including differences in microhabitats, sensory adaptations, and/or random evolutionary history. Future work incorporating specimens across multiple populations with allopatric and sympatric *P. truei* and *P. californicus* as well as dietary manipulation will elucidate whether the relationship between craniomandibular and dietary differences arose through adaptations toward different morphological optima or through developmental plasticity in which different dietary items influenced the development of the skull and mandible.

Acknowledgements We thank the many mentors, staff, and students of the University of California, Santa Cruz (UCSC) Small Mammal Undergraduate Research in the Forest (SMURF) program who have worked with us and taught us about the natural history of deer mice. We would like to thank Tina Cheng (UCSC), Karen Holl (UCSC), and Gage H. Dayton (UCSC) for their support of this study.

Funding Funding for the SMURF program was provided by the UCSC Department of Ecology and Evolutionary Biology, the Webster Chair Fund, the Kenneth S. Norris Center for Natural History, and the UC Natural Reserve System. CJL was funded by a National Science Foundation Graduate Research Fellowship.

References

Adams DC, Otárola-Castillo E (2013) Geomorph: an r package for the collection and analysis of geometric morphometric shape data. Methods Ecol Evol 4:393–399

Alfaro ME, Bolnick DI, Wainwright PC (2005) Evolutionary consequences of many-to-one mapping of jaw morphology to mechanics in labrid fishes. Am Nat 165:E140–E154

Anderson MJ (2001) A new method for non-parametric multivariate analysis of variance. Austral Ecol 26:32–46

Anderson RA, McBrayer LD, Herrel A (2008) Bite force in vertebrates: opportunities and caveats for use of a nonpareil whole-animal performance measure. Biol J Linn Soc 93:709–720

Bookstein FL (1997) Landmark methods for forms without landmarks: morphometrics of group differences in outline shape. Med Image Anal 1:225–243

Bulté G, Irschick DJ, Blouin-Demers G (2008) The reproductive role hypothesis explains trophic morphology dimorphism in the northern map turtle. Funct Ecol 22:824–830

Collar DC, Reece JS, Alfaro ME, Wainwright PC (2014) Imperfect morphological convergence: variable changes in cranial structures underlie transitions to durophagy in moray eels. Am Nat 183:E168–E184

Cox PG (2008) A quantitative analysis of the Eutherian orbit: correlations with masticatory apparatus. Biol Rev 83:35–69

Dayan T, Simberloff D (1994) Character displacement, sexual dimorphism, and morphological variation among British and Irish mustelids. Ecology 75:1063–1073

Druzinsky RE (2010) Functional anatomy of incisal biting in Aplodontia rufa and sciuromorph rodents—part 2:

sciuromorphy is efficacious for production of force at the incisors. Cells Tissues Organs 192:50–63
Ferry-Graham LA, Bolnick DI, Wainwright PC (2002) Using functional morphology to examine the ecology and evolution of specialization. Integr Comp Biol 42:265–277
Goodall C (1991) Procrustes methods in the statistical analysis of shape. J R Stat Soc Ser B Stat Methodol 53:285–339
Grant PR, Grant BR (2002) Unpredictable evolution in a 30-year study of Darwin's finches. Science 296:707–711
Herrel A, Damme RV, Vanhooydonck B, Vree FD (2001) The implications of bite performance for diet in two species of lacertid lizards. Can J Zool 79:662–670
Herrel A, Joachim R, Vanhooydonck B, Irschick DJ (2006) Ecological consequences of ontogenetic changes in head shape and bite performance in the Jamaican lizard *Anolis lineatopus*. Biol J Linn Soc 89: 443–454
Holmes MW, Boykins GKR, Bowie RCK, Lacey EA (2015) Cranial morphological variation in *Peromyscus maniculatus* over nearly a century of environmental change in three areas of California. J Morpho 277:96–106
Kalcounis-Rüppell MC, Millar JS (2002) Partitioning of space, food, and time by syntopic *Peromyscus boylii* and *P californicus*. J Mammal 83:614–625
Kardong KV (2014) Vertebrates: comparative anatomy, function, evolution Boston: McGraw-Hill Education
Kaufman DW, Kaufman GA (1989) Population biology. In: Kirkland G, Layne J (Eds) Advances in the study of *Peromyscus* Rodentia. Lubbock, pp 233–271
La Croix S, Holekamp KE, Shivik JA, Lundrigan BL, Zelditch ML (2011) Ontogenetic relationships between cranium and mandible in coyotes and hyenas. J Morpho 272:662–674
Law CJ, Venkatram V, Mehta RS (2016a) Sexual dimorphism in craniomandibular morphology of southern sea otters (*Enhydra lutris nereis*). J Mammal 97:1764–1773
Law CJ, Young C, Mehta RS (2016b) Ontogenetic scaling of theoretical bite force in southern sea otters (*Enhydra lutris nereis*). Physiol Biochem Zool 89:347–363
Maestri R, Patterson BD, Fornel R, Monteiro LR, Freitas TRO (2016) Diet, bite force and skull morphology in the generalist rodent morphotype. J Evol Biol 29:2191–2204
Maki K, Nishioka T, Shioiri E, Angle TTT (2002) Effects of dietary consistency on the mandible of rats at the growth stage: computed X-ray densitometric and cephalometric analysis. Angle Orthod 72: 468–475
Mori A, Vincent SE (2008) An integrative approach to specialization: relationships among feeding morphology, mechanics, behaviour, performance and diet in two syntopic snakes. J Zool 275:47–56
Myers P, Gillespie BW, Zelditch ML (1996) Phenotypic plasticity in skull and dental morphology in the prairie deer mouse (*Peromyscus maniculatus bairdii*). J Morpho 229:229–237
Pfaller JB, Gignac PM, Erickson GM (2011) Ontogenetic changes in jaw-muscle architecture facilitate durophagy in the turtle *Sternotherus minor*. J Exp Biol 214:1655–1667
Pianka ER (1973) The structure of lizard communities. Annu Rev Ecol Syst 4:53–74
R Core Team (2017) R: A language and environment for statistical computing
Reid REB, Greenwald EN, Wang Y, Wilmers CC (2013) Dietary niche partitioning by sympatric *Peromyscus boylii* and *P. californicus* in a mixed evergreen forest. J Mammal 94:1248–1257
Rohlf FJ (2005) TpsDig, digitize landmarks and outlines, version 25 Department of Ecology and Evolution, State University of New York at Stony Brook New York, USA, Available at: http://life.bio.sunysb.edu/ee/rohlf/software.html
Rohlf FJ, Slice D (1990) Extensions of the Procrustes method for the optimal superimposition of landmarks. Syst Zool 39:40–21
Root RB (1967) The niche exploitation pattern of the blue-gray gnatcatcher. Ecol Monogr 37:317–350
Santana SE, Dumont E, Davis JL (2010) Mechanics of bite force production and its relationship to diet in bats. Funct Ecol 24:776–784
Schlager S (2016) Morpho: calculations and visualisations related to Geometric Morphometrics R-package version 24
Schoener TW (1974) Resource partitioning in ecological communities. Science 185:27–39
Smartt RA (1978) A comparison of ecological and morphological overlap in a *Peromyscus* community. Ecology 59:216–220
Tanner JB, Zelditch ML, Lundrigan BL (2010) Ontogenetic change in skull morphology and mechanical advantage in the spotted hyena (*Crocuta crocuta*). J Morpho 271:353–365
Timm-Davis LL, DeWitt TJ, Marshall CD (2015) Divergent skull morphology supports two trophic specializations in otters (Lutrinae). PLoS One 10:e0143236–e0143218
Turnbull WD (1970) Mammalian masticatory apparatus Field Museum of Natural History
van der Meij MAA, Bout RG (2006) Seed husking time and maximal bite force in finches. J Exp Biol 209:3329–3335
Verwaijen D, Van Damme R, Herrel A (2002) Relationships between head size, bite force, prey handling efficiency and diet in two sympatric lacertid lizards. Funct Ecol 16:842–850
Wainwright PC (1991) Ecomorphology: experimental functional anatomy for ecological problems. Amer Zool 31:680–693
Wainwright PC, Alfaro ME, Bolnick DI, Hulsey CD (2005) Many-to-one mapping of form to function: a general principle in organismal design? Integr Comp Biol 45:256–262
Watt DG, Williams CHM (1951) The effects of the physical consistency of food on the growth and development of the mandible and the maxilla of the rat. Am J Orthod 37:895–928
Žagar A, Carretero MA, Vrezec A, Drašler K, Kaliontzopoulou A (2017) Towards a functional understanding of species coexistence: ecomorphological variation in relation to whole-organism performance in two sympatric lizards. Funct Ecol 211:1336–1312
Zelditch ML, Swiderski DL, Sheets HD (2012) Geometric morphometrics for biologists: a primer Academic Press